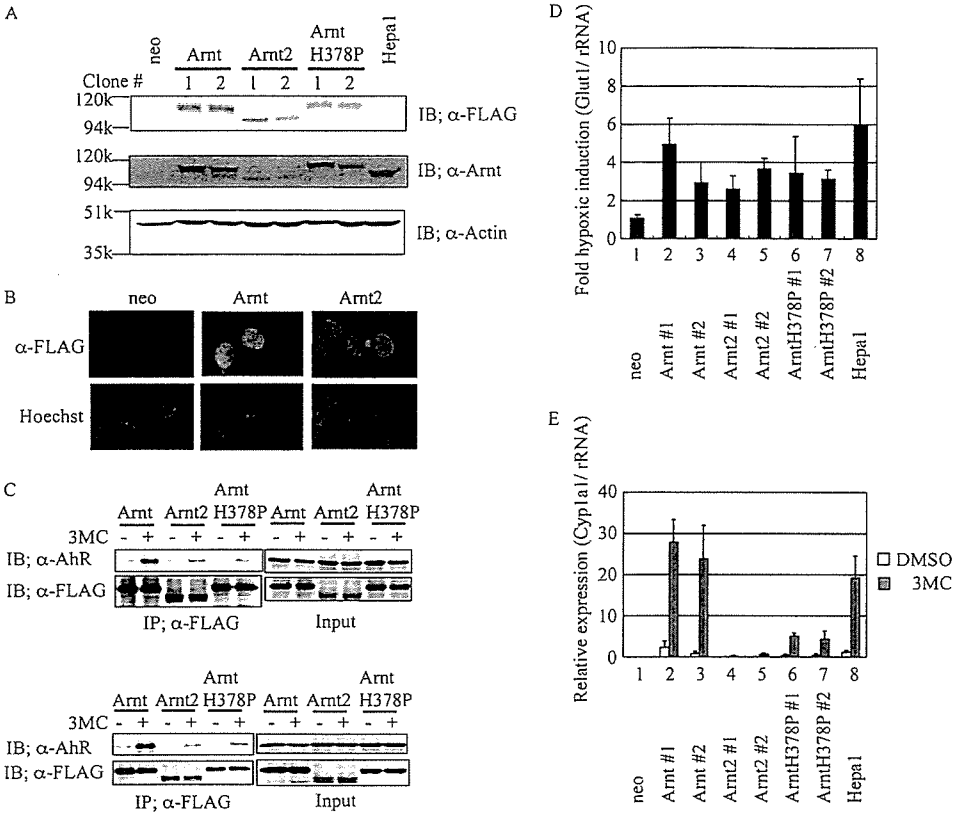

FIGURE 4. **Transcriptional activities of Arnt, Arnt2 and ArntH378P mutant in stably transformed Hepa1-c4 cells.** *A*, expression of 3xFLAG-Arnt, -Arnt2, and -ArntH378P. Expressed proteins were assessed by Western blotting (*IB*, immunoblot) using anti-Arnt, anti-FLAG, and anti-actin antibodies. *B*, cellular localization of 3xFLAG-Arnt and 3xFLAG-Arnt2. Hepa1-c4 cells stably expressing 3xFLAG-Arnt and 3xFLAG-Arnt2 were fixed and immunostained for Arnt and Arnt2 with anti-FLAG antibody. *C*, coimmunoprecipitation of AhR with Arnt, Arnt2, and ArntH378P in response to 3MC. Whole cell extracts of transformants expressing 3xFLAG-Arnt, 3xFLAG-Arnt2, and 3xFLAG-ArntH378P treated with 3MC or Me_2SO (dimethyl sulfoxide (*DMSO*)) were coimmunoprecipitated by anti-FLAG antibody. Coimmunoprecipitation and Western blotting were performed by the methods described under "Experimental Procedures." The *top* and *bottom left panels* show AhR and 3xFLAG-Arnts proteins coimmunoprecipitated by anti-FLAG antibody. *Input* is shown in the *right panels*. The *upper* and *lower panels* represent clone 1 and clone 2, respectively. *D*, expression of endogenous *Glut-1* gene in transformants expressing 3xFLAG-Arnt, -Arnt2, and -ArntH378. Transformed Hepa1-c4 cells were cultured for 16 h under conditions of normoxia or hypoxia (1% O_2), and cell extracts were prepared and used for determination of Glut-1 mRNA expression by real-time PCR analysis. Values are normalized against those for rRNA, and the results are expressed as induction ratios of hypoxic to normoxic activities. *E*, Expression of endogenous *CYP1A1* gene in the transformants. Stably transformed Hepa1-c4 cells were treated with Me_2SO or 3MC for 18 h, and the cell extracts were prepared and used for determination of CYP1A1 mRNA by real-time PCR analysis.

the Arnt His-to-Pro mutant induced luciferase expression to the same extent in response to hypoxia (Fig. 3*B*, *lower panel*). These data indicate that a single amino acid change is mainly responsible for the differential binding of Arnt and Arnt2 with AhR, whereas both Arnt and Arnt2 are equally capable of binding with HIFα.

Physical Interaction and Transcriptional Activity of Arnt and Arnt2 with AhR in Stable Transformants—Up to this point, we have studied the activity and interactions of WT Arnt and Arnt2 and their mutants with AhR and HIFα using relatively artificial transient transfection and two-hybrid assays. We wanted to examine the behavior of these proteins in a more physiologic setting, and we generated Hepa1-c4 cells stably expressing 3xFLAG-Arnt, -Arnt2, and -ArntH378P as described under "Experimental Procedures."

For each construct we isolated two clones with 3xFLAG-Arnt/Arnt2 expression levels comparable with endogenous Arnt in unmodified Hepa1 cells (Fig. 4*A*) and the stably expressed 3xFLAG-Arnt, -Arnt2, and -ArntH378P (data not shown) proteins localized to the nucleus (Fig. 4*B*) (28). To evaluate the interaction between endogenous AhR and these stably expressed 3xFLAG-Arnt, -Arnt2, and -ArntH378P proteins, AhR-3xFLAG-Arnt coimmunoprecipitation assays were performed. In the absence of cellular treatment with 3MC, AhR was not coimmunoprecipitated with 3xFLAG-tagged Arnt, Arnt2, or ArntH378P by an anti-FLAG antibody. However, following incubation of cells with 3MC, AhR was coimmunoprecipitated with 3xFLAG-Arnt by using anti-FLAG antibody, but only a small amount of AhR was detected in the anti-FLAG immunoprecipitates from two transformant cell lines expressing 3xFLAG-Arnt2 or 3xFLAG-ArntH378P (Fig. 4*C*). These results are consistent with the reduced affinity of Arnt2 or the ArntH378P mutant for AhR as revealed in the mammalian two-hybrid system (Fig. 3*B*, *top panel*, *columns 1*, *7*, and *8*), but they are at odds with a previous study from our laboratory (13). In that report, we incubated *in vitro* translated Arnt and Arnt2 with AhR produced in Sf2 cells. It is likely that the relatively high concentrations of Arnt2 and AhR produced in the *in vitro* incubation system gave rise to a misleadingly significant band.

We next investigated the transcriptional activity of Arnt, Arnt2, and the ArntH378P mutant in the generated stable transformant cells, and we chose to examine Glut-1 and CYP1A1 induction by quantitative real-time PCR as target genes for HIF1α and AhR, respectively (29, 30). In cells expressing 3xFLAG-Arnt, -Arnt2, or -ArntH378P, Glut-1 was induced to a similar extent under hypoxic conditions when mRNA levels were normalized to normoxic cells (Fig. 4*D*). In contrast, treatment of cells stably expressing 3xFLAG-Arnt with 3MC dramatically increased CYP1A1 mRNA levels compared with untreated cells, and little induction was seen in cells expressing 3xFLAG-Arnt2 (Fig. 4*E*). Cells expressing 3xFLAG-ArntH378P slightly, but significantly, increased CYP1A1 mRNA levels following 3MC treatment, indicating that His-378 in the Arnt PASB domain strongly influences Arnt binding to AhR but that other regions of Arnt also contribute to AhR binding.

The Arnt PASA and PASB Domains Cooperatively Bind AhR—We saw some degree of *CYP1A1* transcription in response to 3MC in cells expressing 3xFLAG-ArntH378P, and we were

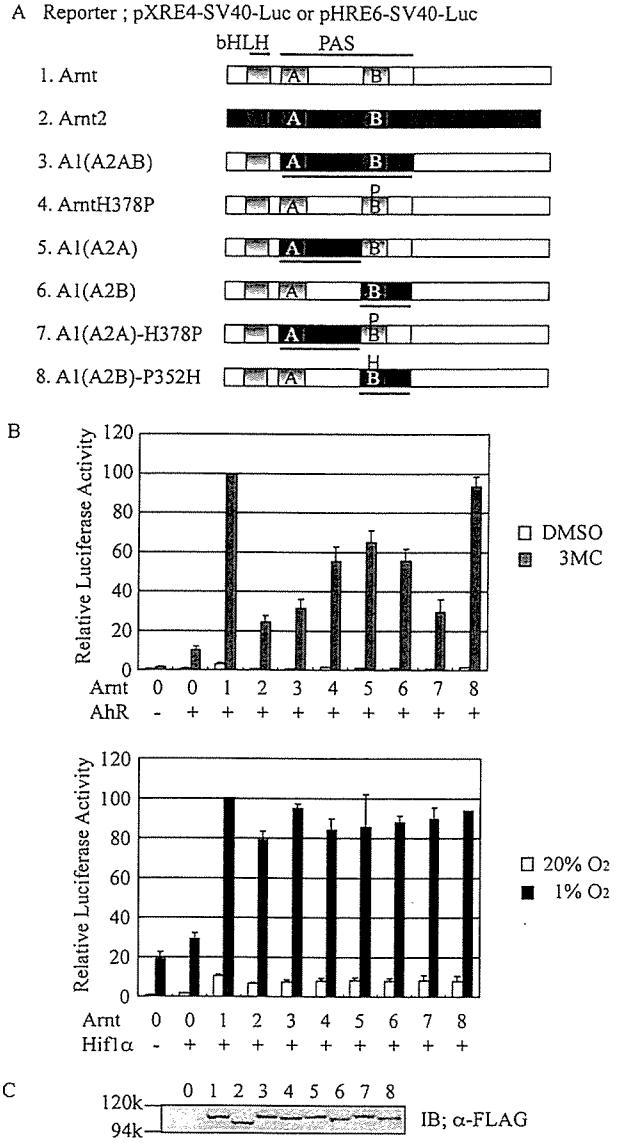

FIGURE 5. **Contribution of PASA and PASB sequences of full-length Arnt and Arnt2 to the expression of XRE-driven and HRE-driven reporter genes.** *A*, constructs of the expression plasmids of Arnt and Arnt2 and their chimeric and mutant proteins. *Underlines* show the Arnt domain replaced by the corresponding Arnt2 domain (*constructs 3* and *5–8*). *B, top*, expression of the XRE-driven reporter gene. HeLa cells were transfected with 10 ng of pXRE4-SV40-Luc, 2 ng of the indicated expression plasmid, and 20 ng of pBOSmAhR, and the reporter gene expression assay was performed as described in the legend to Fig. 1*B*. *DMSO*, dimethyl sulfoxide (Me_2SO). *Bottom*, expression of the HRE-driven reporter gene. HeLa cells were transfected with 10 ng of pHRE6-SV40-Luc, 2 ng of the indicated expression plasmid, and 20 ng of pBOShHIF1α, and the reporter gene expression assay was performed as described in the legend to Fig. 1*B*. Values are represented by mean ± S.D. of the results of three independent experiments normalized to *Renilla* luciferase activity used as an internal control. The full activity of *column 1* was taken as a standard to calculate relative activities. *C*, concentrations of the expressed effector proteins. The cells were transfected with 10 ng of the indicated expression construct in 6-well plates. Equal amounts of cell lysates were used for determination of the expressed proteins. *Columns* in *B* and *C*: *0*, pBOS; *1*, pBOS3xFLAG-Arnt; *2*, pBOS3xFLAG-Arnt2; *3*, pBOS3xFLAG-A1(A2AB); *4*, pBOS3xFLAG-ArntH378P; *5*, pBOS3x-FLAG-A1(A2A); *6*, pBOS3xFLAG-A1(A2B); *7*, pBOS3xFLAG-A1(A2A)H378P; *8*, pBOS3xFLAG-A1(A2B)P352H. *IB*, immunoblot.

interested in determining other regions of Arnt that support its interaction with AhR. Toward this end, we generated several additional Arnt/Arnt2 chimeric constructs (Fig. 5*A*) and investigated their ability to interact with AhR by luciferase reporter assay. As shown above, all WT and chimeric Arnt and Arnt2 constructs were able to induce luciferase expression in response to hypoxia when coexpressed with HIF1α (Fig. 5*B*, *lower panel*). As expected, Arnt induced XRE-driven luciferase expression to a greater extent than Arnt2, but some luciferase expression was seen in Arnt2-expressing cells compared with untreated cells as reported in our previous study (13) (Fig. 5*B*, *upper panel, columns 0, 1*, and *2*). The physiologic significance of this induction is questionable, however, given the inability of stably expressed Arnt2 to induce the expression of the endogenous *CYP1A1* gene (Fig. 4*E*, *columns 4* and *5*); the ability of Arnt2 to induce luciferase in response to 3MC may be an overexpression artifact. Substitution of the Arnt PASA and PASB domains with those of Arnt2 led to reduced luciferase expression comparable with WT Arnt2 (Fig. 5*B*, *upper panel, columns 2*, and *3*). Additionally, the H378P mutation as well as swapping the PASA or PASB domain of Arnt2 led to intermediate levels of luciferase expression (Fig. 5*B*, *upper panel, columns 4, 5*, and *6*), indicating that the PASA domain is largely responsible for the additional AhR binding activity of Arnt. Interestingly, replacement of the Arnt PASA domain with that of Arnt2 and mutation of His-378 to Pro led to luciferase expression comparable with that of WT Arnt2 (column 7), thus confirming the importance of the two regions for Arnt·AhR binding. In contrast, when the Pro residue of the Arnt2 PASB domain was mutated to His, and this mutant PASB domain replaced the corresponding one in Arnt, luciferase expression in response to 3MC was restored to WT Arnt levels (Fig. 5*B*, *upper panel, column 8*). As expected from the two-hybrid assay, all WT and chimeric Arnt/Arnt2 constructs behaved similarly in response to hypoxia (Fig. 5*B*, *lower panel*).

The PASB Domain of AhR Is Responsible for Differential Binding to Arnt and Arnt2—A single amino acid change largely impaired the ability of Arnt to bind AhR, and we determined the region of AhR that interacts with Arnt PASB. We used a mammalian two-hybrid system with GAL4DBD-fused Arnt, Arnt2, and the Arnt mutant as bait (Fig. 3*A*, *constructs 1, 7*, and *8*). When we used VP16AD-AhRΔC (Fig. 6*A*) as prey together with GAL4DBD-Arnt-bHLHPAS, the reporter gene was strongly induced following 3MC treatment (Fig. 6*B*, *column 4*). Expression of a VP16AD-AhRΔBΔC construct (Fig. 6*A*) further lacking the AhR PASB region constitutively expressed a high degree of luciferase activity, although a slight inducibility remained with 3MC (Fig. 6*B*, *column 5*). The PASB region of AhR binds the HSP90 complex, and in its absence, AhR is not retained in the cytoplasm and mediates transcription in the absence of stimuli (31–33). In contrast, in cells expressing both GAL4DBD-Arnt2-bHLHPAS and VP16AD-AhRΔC, reporter gene expression was reduced remarkably and was only slightly inducible (Fig. 6*B*, *column 10*). In stark contrast, coexpression of the PASB-deleted construct VP16AD-AhRΔBΔC with GAL4DBD-Arnt2-bHLHPAS led to constitutive luciferase activity comparable with that seen with GAL4DBD-Arnt-bHLHPAS (Fig. 6*B*, *column 5 versus 11*). These results indicate that the bHLH and PASA domains of AhR are able to interact with Arnt and Arnt2 to an equal extent to mediate constitutive transcriptional activity. Addition of the PASB region of AhR, how-

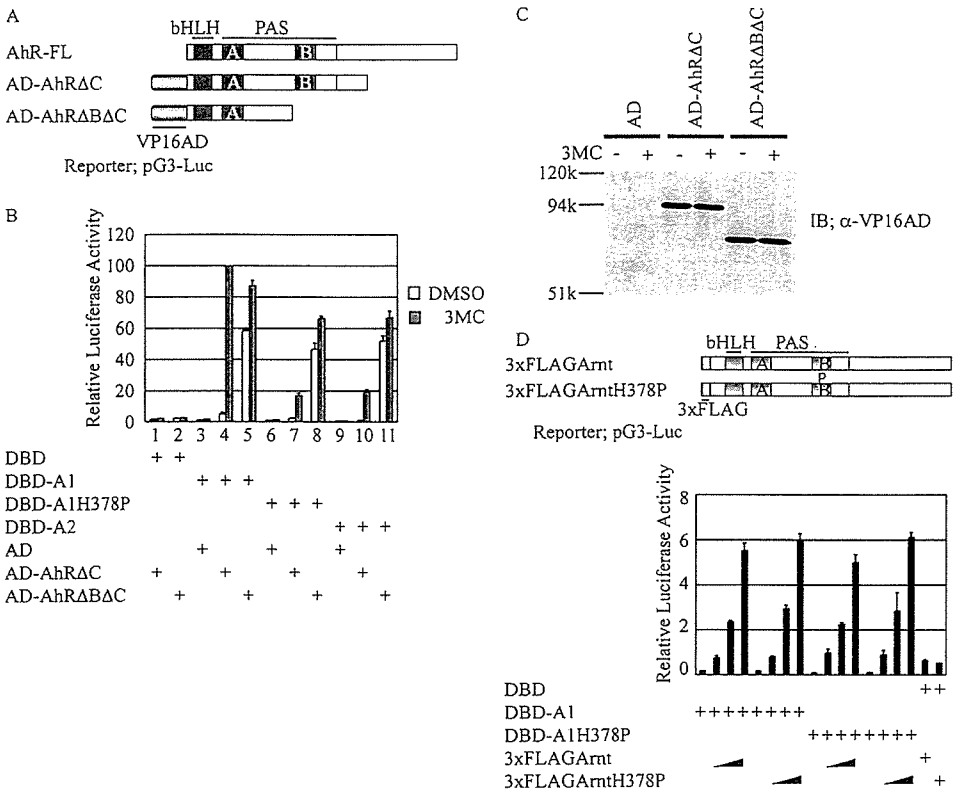

FIGURE 6. **PASB/PASB interaction is important for specific AhR/Arnt heterodimerization.** *A*, constructs of VP16AD-AhRΔC (*AD-AhRΔC*) and VP16AD-AhRΔBΔC (*AD-AhRΔBΔC*) used as prey. *B*, reporter gene expression. 293T cells were transfected with pG3-Luc, the indicated bait plasmid (pBOSGAL4DBD (*DBD*), pBOSGAL4DBD-Arnt-bHLHPAS (*DBD-A1*), pBOSGAL4DBD-ArntH378P-bHLHPAS (*DBD-A1H378P*), or pBOSGAL4DBD-Arnt2-bHLHPAS (*DBD-A2*)), and the indicated prey plasmid (pBOSVP16AD (*AD*), pBOSVP16AD-mAhRΔC, or pBOSVP16AD-mAhRΔBΔC), and after 24 h of incubation, the cells were treated with 1 μM 3MC or Me_2SO (dimethyl sulfoxide (*DMSO*)) for 18 h. Values are represented by mean ± S.D. of the results of three independent experiments normalized to *Renilla* luciferase activity used as an internal control. The full activity of *column 1* was taken as a standard to calculate relative activities. *C*, protein expression. The cells were transfected with 50 ng of the indicated expression construct in 6-well plates. The protein levels of all constructs were evaluated by Western blotting (*IB*, immunoblot) using anti-VP16AD antibody. Equal amounts of cell lysates were used for gel electrophoresis. *Columns 1* and *2*, pBOSVP16AD (*AD*); *columns 3* and *4*, pBOSVP16AD-mAhRΔC (*AD-AhRΔC*); *columns 5* and *6*, pBOSVP16AD-mAhRΔBΔC (*AD-AhRΔBΔC*). In *columns 1, 3*, and *5*, cells were treated with Me_2SO for 18 h; in *columns 2, 4*, and *6*, cells were treated with 1 μM 3MC for 18 h. *D*, effect of H378P mutation on Arnt/Arnt homodimerization. *Top*, 3xFLAG-Arnt and 3xFLAG-ArntH378P were used as activators. *Bottom*, expressed luciferase activities from Arnt/Arnt interaction. 293T cells were transfected with 100 ng of pG3-Luc and 10 ng of the indicated bait vectors (pBOSGAL4DBD, pBOSGAL4DBD-Arnt-bHLHPAS, or pBOSGAL4DBD-ArntH378P-bHLHPAS) and the indicated prey vector (50 ng of pBOS or 10, 20, or 50 ng of pBOS3xFLAG-Arnt or pBOS3xFLAG-ArntH378P). After 24 h of culture, the medium was changed, and the cells were further cultured for 24 h. The cell extracts were prepared from the cultured cells and used for luciferase assays. Values are represented by mean ± S.D. of the results of three independent experiments normalized to *Renilla* luciferase activity used as an internal control.

ever, specifically inhibited its interaction with Arnt2, leading to reduced reporter gene expression. Thus, the PASB domain of AhR determines its binding specificity for Arnt.

We next examined the ability of the His-378 to Pro Arnt mutant to interact with AhR; it behaved virtually identically to Arnt2 (Fig. 6*B*, *columns 7* and *8 versus 10* and *11*), indicating that Pro-352 in Arnt2 is primarily responsible for its reduced affinity for AhR. In these experiments, the prey proteins were expressed almost equally (Fig. 6*C*).

Homodimerization of Arnt and Arnt H378P—Arnt can form a heterodimer with AhR and HIF1α, but it also homodimerizes and binds E-box sequences (25, 34, 35). We investigated the ability of ArntH378P to homodimerize with either WT or mutant Arnt, using the mammalian two-hybrid assay with GAL4DBD-Arnt-bHLHPAS or GAL4DBD-ArntH378P-bHLHPAS as bait (Fig. 3*A*, *constructs 1* and *7*) and a full-length 3xFLAG-Arnt or its H378P mutant as prey (Fig. 5*A*, *constructs 1* and *4*). In any combination of bait and prey, both WT and H378P mutant Arnt activated similar levels of reporter gene expression (Fig. 6*D*), indicating that Arnt homodimerization is not sensitive to the H378P mutation. This result also suggests that Arnt PASB His-to-Pro mutation influences specifically AhR-Arnt dimerization, not the general dimerization.

DISCUSSION

Arnt and Arnt2 are structurally very similar and are believed to be common obligate dimerization partners for a number of bHLH-PAS transcription factors including AhR, HIFα, and Sims (13). We found no differences in the ability of Arnt, Arnt2, or any mutant or chimeric constructs used to activate gene expression in response to hypoxia in both transient and stable expression systems, suggesting that both proteins are equally able to bind HIFα, the key transcription factor mediating the hypoxic response. Thus, Arnt and Arnt2 play functionally interchangeable and overlapping roles in glycolysis, erythropoiesis, and angiogenesis in response to hypoxic conditions. The compensatory effects of Arnt and Arnt2 are noticeable in central nervous system development where Arnt2 is expressed abundantly (36, 37). Whole-mount PECAM (platelet endothelial cell adhesion molecule) immunohistochemistry on the embryonic central nervous system revealed no obvious differences between the WT and Arnt2$^{-/-}$ embryos, whereas Arnt$^{-/-}$ embryos had clear disruptions of the vascular endothelial network (20). This observation suggests that the expression of *VEGF* and other HIFα target genes in Arnt2$^{-/-}$ embryos is effectively normal, presumably because of the compensatory effects of Arnt. In the later stage of central nervous system development, however, several unique functions of Arnt2 become apparent, and Arnt2$^{-/-}$ embryos die perinatally with impaired hypothalamic development (15).

In contrast to their overlapping ability to bind HIFα, and also in apparent contrast with a previous report (13), clear differences were seen in the ability of Arnt and Arnt2 to interact with AhR. XRE-driven luciferase activity in cells expressing Arnt2 was much less than that seen in cells expressing Arnt following

3MC treatment, and the transcription of an XRE-responsive endogenous gene, *CYP1A1*, was completely absent in Hepa1-c4 cells stably expressing Arnt2 after treatment with 3MC (Fig. 4*E*, *columns 4* and *5*). In contrast, Hepa1-c4 cells stably expressing Arnt induced high levels of *CYP1A1* transcripts following 3MC treatment (Fig. 4*E*, columns 2 and 3). Some activation of the XRE-driven reporter gene by Arnt2 (about one-fifth of the Arnt activation) in the previous report (13) is misleading, most probably because of overexpression of Arnt2 in the transient DNA transfection experiments. Arnt2 expressed in these transformant cells was clearly functional, as shown by its ability to induce HRE-responsive genes in conjunction with HIFα (Fig. 4*D*), suggesting that Arnt2 plays little or no role in the cellular response to xenobiotics to induce the XRE-inducible genes in conjunction with AhR. This conclusion is further supported by the observation that zebrafish injected with a zfArnt2 antisense morpholino induced zfCYP1A1 in response to TCDD- as well as sham-treated animals, and there were no differences in TCDD-induced cytotoxicities requiring Arnt/AhR dimerization, such as pericardial edema, reduced trunk blood flow, and shortened lower jaw between these animals (38).

The bHLH domain of AhR is thought to be essential for heterodimer formation between bHLH-PAS transcription factors, and the bHLH domain alone of AhR is capable of dimerizing with the unrelated bHLH-Zip transcription factor USF (39). When the PASA domain is added to the AhR bHLH domain, however, AhR becomes much less promiscuous and stably binds Arnt (39). We showed that a construct consisting of the AhR bHLH and PASA domains binds both Arnt and Arnt2 (Fig. 6*B*, *columns 5* and *11*), but the addition of the PASB domain restricts AhR binding exclusively to Arnt (Fig. 6*B*, *columns 4* and *10*). Taken together, these data indicate that Arnt2 is not likely involved in the induction of drug-metabolizing enzymes following exposure to exogenous aromatic chemicals and other biological processes requiring AhR as a transcription factor.

A recent study reported that both the PASA and PASB domains of HIFα are necessary for heterodimer formation with Arnt (40). The minimal PAS domain structure consists of a 3-stranded β sheet, designated the β-scaffold, and a central α-helical PAS core region containing three short stretches of α-helices and β-sheets connected by a single α-helix called the helical connector. Mutational analysis revealed that hydrophobic interactions between conserved amino acids on the surface of the β-scaffold of HIFα and Arnt are important for heterodimerization, and replacement of hydrophilic amino acids (Q322E, M338E, and Y342T in HIF2α) disrupted this interaction leading to reduced transcription activity in response to hypoxia (40–42). Replacement of His-378 with Pro in Arnt, a residue a little away from the β-scaffold, disrupted its interaction with AhR but had no effect on the interaction of Arnt with HIFα. This suggests that the PASB/PASB-interacting surfaces or modes of AhR and Arnt are different from those of HIFα and Arnt. Additionally, the structural basis for the inhibition of AhR binding by Pro-352 of Arnt2, without affecting HIFα binding, should be examined. Such studies could provide valuable insight into the molecular regulation of the xenobiotic response as well as the diversification of a highly conserved family of transcription factors.

Acknowledgments—We thank Dr. O. Hankinson for kindly providing Hepa1-c4 mutant and Y. Nemoto for clerical work.

REFERENCES

1. Jackson, F. R., Bargiello, T. A., Yun, S. H., and Young, M. W. (1986) *Nature* **320,** 185–188
2. Reddy, P., Jacquier, A. C., Abovich, N., Petersen, G., and Rosbash, M. (1986) *Cell* **46,** 53–61
3. Hoffman, E. C., Reyes, H., Chu, F. F., Sander, F., Conley, L. H., Brooks, B. A., and Hankinson, O. (1991) *Science* **252,** 954–958
4. Crews, S. T., Thomas, J. B., and Goodman, C. S. (1988) *Cell* **52,** 143–151
5. Nambu, J. R., Lewis, J. O., Wharton, K. A., Jr., and Crews, S. T. (1991) *Cell* **67,** 1157–1167
6. Kewley, R. J., Whitelaw, M. L., and Chapman-Smith, A. (2004) *Int. J. Biochem. Cell Biol.* **36,** 189–204
7. Schmidt, J. V., Su, G. H., Reddy, J. K., Simon, M. C., and Bradfield, C. A. (1996) *Proc. Natl. Acad. Sci. U. S. A.* **93,** 6731–6736
8. Baba, T., Mimura, J., Nakamura, N., Harada, N., Yamamoto, M., Morohashi, K., and Fujii-Kuriyama, Y. (2005) *Mol. Cell. Biol.* **25,** 10040–10051
9. Huang, L. E., Gu, J., Schau, M., and Bunn, H. F. (1998) *Proc. Natl. Acad. Sci. U. S. A.* **95,** 7987–7992
10. Ryan, H. E., Lo, J., and Johnson, R. S. (1998) *EMBO J.* **17,** 3005–3015
11. Iyer, N. V., Kotch, L. E., Agani, F., Leung, S. W., Laughner, E., Wenger, R. H., Gassmann, M., Gearhart, J. D., Lawler, A. M., Yu, A. Y., and Semenza, G. L. (1998) *Genes Dev.* **12,** 149–162
12. Tian, H., Hammer, R. E., Matsumoto, A. M., Russell, D. W., and McKnight, S. L. (1998) *Genes Dev.* **12,** 3320–3324
13. Hirose, K., Morita, M., Ema, M., Mimura, J., Hamada, H., Fujii, H., Saijo, Y., Gotoh, O., Sogawa, K., and Fujii-Kuriyama, Y. (1996) *Mol. Cell. Biol.* **16,** 1706–1713
14. Drutel, G., Kathmann, M., Heron, A., Schwartz, J. C., and Arrang, J. M. (1996) *Biochem. Biophys. Res. Commun.* **225,** 333–339
15. Hosoya, T., Oda, Y., Takahashi, S., Morita, M., Kawauchi, S., Ema, M., Yamamoto, M., and Fujii-Kuriyama, Y. (2001) *Genes Cells* **6,** 361–374
16. Maltepe, E., Schmidt, J. V., Baunoch, D., Bradfield, C. A., and Simon, M. C. (1997) *Nature* **386,** 403–407
17. Kozak, K. R., Abbott, B., and Hankinson, O. (1997) *Dev. Biol.* **191,** 297–305
18. Adelman, D. M., Gertsenstein, M., Nagy, A., Simon, M. C., and Maltepe, E. (2000) *Genes Dev.* **14,** 3191–3203
19. Abbott, B. D., and Buckalew, A. R. (2000) *Dev. Dyn.* **219,** 526–538
20. Keith, B., Adelman, D. M., and Simon, M. C. (2001) *Proc. Natl. Acad. Sci. U. S. A.* **98,** 6692–6697
21. Mizushima, S., and Nagata, S. (1990) *Nucleic Acids Res.* **18,** 5322
22. Mimura, J., Ema, M., Sogawa, K., and Fujii-Kuriyama, Y. (1999) *Genes Dev.* **13,** 20–25
23. Numayama-Tsuruta, K., Kobayashi, A., Sogawa, K., and Fujii-Kuriyama, Y. (1997) *Eur. J. Biochem.* **246,** 486–495
24. Ema, M., Taya, S., Yokotani, N., Sogawa, K., Matsuda, Y., and Fujii-Kuriyama, Y. (1997) *Proc. Natl. Acad. Sci. U. S. A.* **94,** 4273–4278
25. Sogawa, K., Nakano, R., Kobayashi, A., Kikuchi, Y., Ohe, N., Matsushita, N., and Fujii-Kuriyama, Y. (1995) *Proc. Natl. Acad. Sci. U. S. A.* **92,** 1936–1940
26. Park, S. K., Dadak, A. M., Haase, V. H., Fontana, L., Giaccia, A. J., and Johnson, R. S. (2003) *Mol. Cell. Biol.* **23,** 4959–4971
27. Pellequer, J. L., Wager-Smith, K. A., Kay, S. A., and Getzoff, E. D. (1998) *Proc. Natl. Acad. Sci. U. S. A.* **95,** 5884–5890
28. Eguchi, H., Ikuta, T., Tachibana, T., Yoneda, Y., and Kawajiri, K. (1997) *J. Biol. Chem.* **272,** 17640–17647
29. Wood, S. M., Gleadle, J. M., Pugh, C. W., Hankinson, O., and Ratcliffe, P. J. (1996) *J. Biol. Chem.* **271,** 15117–15123
30. Ko, H. P., Okino, S. T., Ma, Q., and Whitlock, J. P., Jr. (1996) *Mol. Cell. Biol.* **16,** 430–436
31. Coumailleau, P., Poellinger, L., Gustafsson, J. A., and Whitelaw, M. L. (1995) *J. Biol. Chem.* **270,** 25291–25300
32. Whitelaw, M. L., Gottlicher, M., Gustafsson, J. A., and Poellinger, L. (1993) *EMBO J.* **12,** 4169–4179

33. McGuire, J., Okamoto, K., Whitelaw, M. L., Tanaka, H., and Poellinger, L. (2001) *J. Biol. Chem.* **276,** 41841–41849
34. Antonsson, C., Arulampalam, V., Whitelaw, M. L., Pettersson, S., and Poellinger, L. (1995) *J. Biol. Chem.* **270,** 13968–13972
35. Huffman, J. L., Mokashi, A., Bachinger, H. P., and Brennan, R. G. (2001) *J. Biol. Chem.* **276,** 40537–40544
36. Jain, S., Maltepe, E., Lu, M. M., Simon, C., and Bradfield, C. A. (1998) *Mech. Dev.* **73,** 117–123
37. Aitola, M. H., and Pelto-Huikko, M. T. (2003) *J. Histochem. Cytochem.* **51,** 41–54
38. Prasch, A. L., Heideman, W., and Peterson, R. E. (2004) *Toxicol. Sci.* **82,** 250–258
39. Pongratz, I., Antonsson, C., Whitelaw, M. L., and Poellinger, L. (1998) *Mol. Cell. Biol.* **18,** 4079–4088
40. Yang, J., Zhang, L., Erbel, P. J., Gardner, K. H., Ding, K., Garcia, J. A., and Bruick, R. K. (2005) *J. Biol. Chem.* **280,** 36047–36054
41. Erbel, P. J., Card, P. B., Karakuzu, O., Bruick, R. K., and Gardner, K. H. (2003) *Proc. Natl. Acad. Sci. U. S. A.* **100,** 15504–15509
42. Card, P. B., Erbel, P. J., and Gardner, K. H. (2005) *J. Mol. Biol.* **353,** 664–677

Xenobiotica, April 2006; 36(4): 301–314

Taylor & Francis
Taylor & Francis Group

Species differences in hydrolase activities toward OT-7100 responsible for different bioavailability in rats, dogs, monkeys and humans

S. KURIBAYASHI[1,2] N. UEDA[2], S. NAITO[2], H. YAMAZAKI[1], & T. KAMATAKI[1]

[1]*Division of Drug Metabolism, Graduate School of Pharmaceutical Sciences, Hokkaido University, Sapporo, Japan and* [2]*Division of Pharmacology, Drug Safety and Metabolism, Otsuka Pharmaceutical Factory, Inc., Tokushima, Japan*

(Received 16 September 2005)

Abstract

OT-7100 (5-*n*-butyl-7-(3,4,5-trimethoxybenzoylamino)pyrazolo[1,5-a] pyrimidine) is an amide moiety-bearing pyrazolopyrimidine derivative with a potential analgesic effect. To determine the factors responsible for observed species differences in the bioavailability of this drug, human and experimental animal samples were used to investigate *in vitro* microsomal and cytosolic hydrolase activities in the liver and small intestine vis-à-vis the pharmacokinetics of OT-7100. The AUC_{0-t} values of OT-7100 after oral administration in rats, dogs and monkeys were 0.163, 0.0383 and 0.00147 $\mu g\,h\,ml^{-1}$ divided by $mg\,kg^{-1}$, respectively. The bioavailabilities of OT-7100 after oral administration in rats, dogs and monkeys were 36, 17 and 0.3%, respectively. The plasma concentration–time profiles of intravenously administrated OT-7100 in rats, dogs and monkeys were similar. The hydrolase activities toward OT-7100 in liver microsomes or cytosol were approximately similar in rats, dogs, monkeys and humans. In contrast, hydrolase activities of small intestinal microsomes from monkeys were higher (36.1 $ng\,mg\,protein^{-1}\,min^{-1}$) than those of rats, dogs and humans (5.4, 1.4 and 4.3 $ng\,mg\,protein^{-1}\,min^{-1}$, respectively). These results suggest that the primary factor influencing first-pass metabolism for the OT-7100 is enzymatic hydrolysis in the small intestine. This information provides an important index for extrapolating the pharmacokinetics of drugs in humans using studies on monkeys.

Keywords: *Species differences, pyrazolopyrimidine derivative, hydrolysis, bioavailability, small intestine*

Correspondence: S. Kuribayashi, Department of Drug Metabolism, Division of Pharmacology, Drug Safety and Metabolism, Otsuka Pharmaceutical Factory Inc., 115 Tateiwa, Muya-cho, Naruto, Tokushima 772-8601, Japan. Tel: 81-88-685-1151. Fax: 81-88-686-8176. E-mail: kuribasy@otsukakj.co.jp

ISSN 0049-8254 print/ISSN 1366-5928 online
DOI: 10.1080/00498250600571798

Introduction

In vivo preclinical pharmacokinetic studies are a key component of the overall drug discovery and development paradigm. Typically for a given drug candidate, pharmacokinetic data are first available in at least two or three preclinical species, often including rat, dog and/or monkey, well before clinical data emerge. In practice, however, species differences often complicate extrapolation of preclinical species data to the predicted pharmacokinetics of a molecule in humans (Boxenbaum 1980; Lin 1995). It is widely accepted that the liver is the primary site of first-pass metabolism because of both its size and high content of drug-metabolizing enzymes (Thummel et al. 1997). However, it is gradually becoming evident that metabolizing enzymes involved in the process of absorption in the small intestine also play a crucial role, in some cases, in metabolizing drugs delivered orally (Satoh and Hosokawa 1998; Lin et al. 1999). For example, both hepatic and intestinal enzymes have been implicated in the first-pass metabolism of midazolam after oral administration (Thummel et al. 1996). Differences between humans and experimental animals in the bioavailability of an active metabolite from glycovir arose from differences in the hydrolysis rate of glycovir within the small intestinal mucosa (Cook et al. 1995). Furthermore, there is insufficient predictive accuracy in scale-up estimation even when results from drug studies in monkeys are used to extrapolate to humans (Inaba et al. 1998). Therefore, it is important to investigate species differences/similarities with respect to intestinal drug-metabolizing enzymes in humans and experimental animals in order to improve one's understanding of bioavailability.

Drug-metabolizing enzymes such as cytochrome P450 (CYP) (Zhang et al. 1999; Hashizume et al. 2001) and carboxylesterases (Campbell et al. 1987; Satoh 1987), which are involved in phase I reactions, are present in high concentrations in the small intestine. Hepatic CYP3A4 has been involved in the oxidative metabolism of many drugs (Fitzsimmons and Collins 1997). In contrast, carboxylesterases are important for the hydrolysis of many exogenous compounds, resulting in both activation of prodrugs and inactivation of drugs (Hosokawa et al. 1995; Satoh and Hosokawa 1998). Marked interspecies variations in carboxylesterase activity exist in the small intestine and liver, and there are significant differences in substrate specificity of the various carboxylesterase isoforms (Inoue et al. 1979; Hosokawa et al. 1990). However, since this has not been systematically studied based on chemical structure, there is little information about species differences/similarities between human and monkey carboxylesterases. Therefore, it is difficult to predict the metabolism and pharmacokinetics of drugs in humans based on animal studies.

OT-7100 (5-*n*-butyl-7-(3,4,5-trimethoxybenzoylamino)pyrazolo[1,5-a] pyrimidine) is a pyrazolopyrimidine derivative with the amide moiety that has a potential analgesic effect (Yasuda et al. 1999, 2001; Miki et al. 2001). The proposed metabolic pathways of OT-7100 in rats and dogs are shown in Figure 1.

The metabolites of OT-7100 included M19 and M5, which are hydrolysate of the amide moiety of OT-7100, and M1–3, which result from oxidization of the *n*-butyl groups by CYPs (unpublished data). It is believed that the hydrolysis of OT-7100 is responsible for the species differences and that hydrolysis influences the pharmacokinetics and biotransformation of OT-7100, as well as other drugs with the amide moiety (Satoh and Hosokawa 1998). Since the small intestinal carboxylesterases apparently play an important role in the metabolism and biotransformation of orally administered drugs, it is important to investigate the species differences in the hydrolase activity between humans and experimental animals and to identify the contribution of small intestine

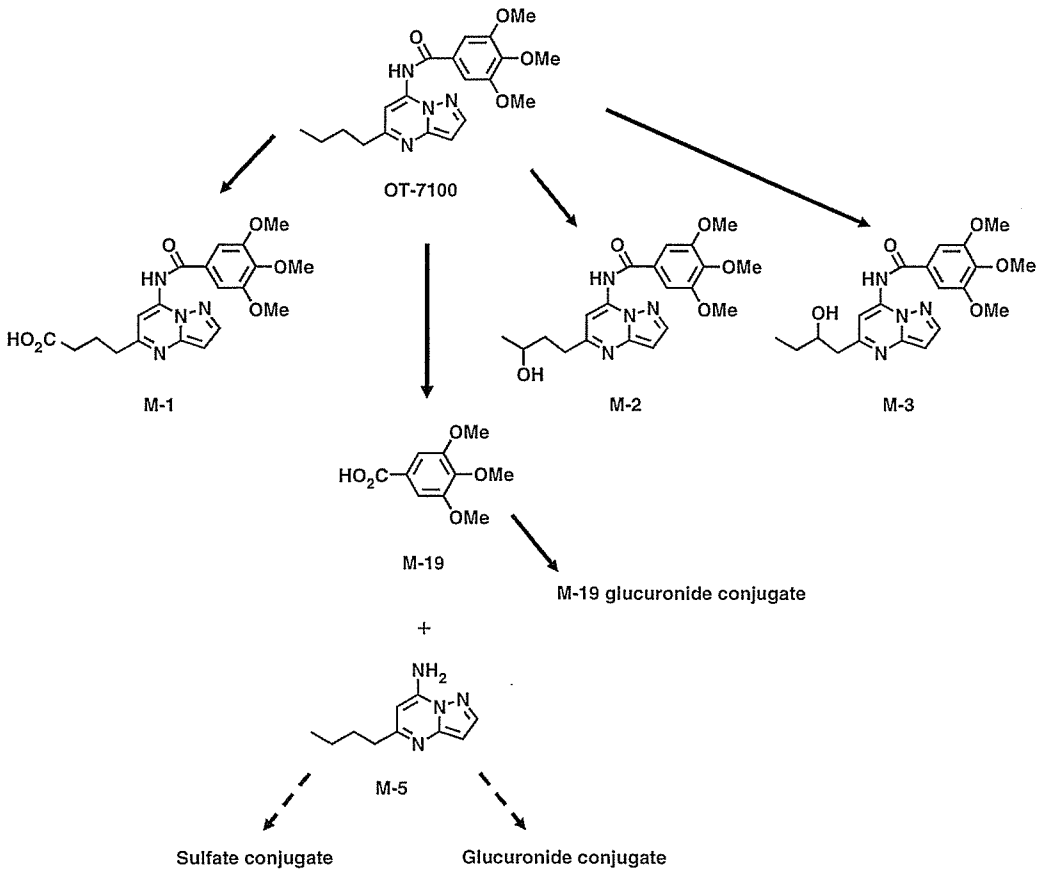

Figure 1. Postulated metabolic pathways of OT-7100 in rats and dogs.

metabolism to the total hydrolysis fraction of an orally administered drug containing the amide moiety.

The present study reports that the different bioavailabilities of the orally administered probe drug OT-7100 with an amide moiety could be accounted for by the differences in specific small intestinal hydrolase activities among humans and experimental animals (rats, dogs and monkeys). It was found that OT-7100 is a good substrate to identify species differences in small intestinal hydrolase activities, particularly between humans and monkeys. The authors have demonstrated that hydrolase activity in the small intestine is one of the primary drug metabolism factors influencing first-pass metabolism in the process of drug absorption.

Materials and methods

Materials

OT-7100 (5-*n*-butyl-7-(3,4,5-trimethoxybenzoylamino)pyrazolo[1,5-a] pyrimidine; molecular weight of 384.44; Figure 1) and its five metabolites (M1–3, M5 and M19) were synthesized at Otsuka Pharmaceutical Factory (Tokushima, Japan). All chemicals

were determined, by reversed-phase HPLC, to be >99.0% pure. All other chemicals and reagents used were of analytical reagent grade.

Animals

Male Sprague–Dawley rats, 6–7 weeks of age, weighing 190–250 g (Charles River Japan, Kanagawa, Japan) and male Beagle dogs, 11–12 months of age, weighing 10.10–10.78 kg (LRE-Strain, HRP, Inc., Kalamazoo, MI, USA) were used. The animals were housed in a room maintained at 23 ± 3°C and at a relative humidity of 55% ± 15%, with an air exchange rate of at least 10 times h^{-1} and a 12-h light/dark cycle. Male cynomolgus monkeys, 3 years of age, weighing approximately 3 kg, were individually housed at the Wakayama Breeding Farm of Keari Co. Ltd (Wakayama, Japan) at 22–26°C and a relative humidity of 45–65%. Animals were fed solid diet (rat; CRF-1, dog; DS-5, monkey; PS, Oriental Yeast Co. Ltd, Tokyo, Japan) once daily and allowed free access to tap water. These studies were approved by the Committee on the Care and Use of Laboratory Animals for the Otsuka Pharmaceutical Factory, Inc, and we followed guidelines similar to those provided in the Guide for the Care and Use of Laboratory Animals (National Research Council, USA).

Preparation of subcellular fractions

Dog, monkey and human liver microsomes and cytosol from three individuals were purchased from KAC Corp (Kyoto, Japan). Rat liver microsomes and cytosol were prepared from three animals. Male rats (Sprague–Dawley, 7 weeks old) were purchased from Charles River Japan. A 3 × volume 0.15 M KCl containing 10 mM EDTA 2Na (adjusted at pH 7.4 using 0.15 M KOH and 0.15 M HCl) was added to the liver and homogenized in an ice bath. The homogenate was centrifuged at 9000*g* for 20 min at 4°C, and an aliquot of the supernatant was further centrifuged at 105 000*g* for 60 min at 4°C. The supernatant, cytosol, was stored at −80°C until use. The remaining pellet fractions were collected, suspended again with 10 ml 100 mM potassium phosphate buffer (pH 7.4) containing 20% glycerol and 1 mM EDTA 2Na, and stored at −80°C until use.

Dog, monkey and human small intestinal microsomes and cytosol from three individuals were purchased from KAC Corp (Kyoto, Japan). One lot of rat small intestinal microsomes and cytosol were prepared from five animals. Male rats (Sprague–Dawley, 7 weeks old) were purchased from Charles River Japan. The small intestine was collected and the inner-side of small intestine was washed with 50 ml ice-cold physiological salt solution. The residual washing solution was then removed from outside the small intestine. The small intestine was incised and the mucosa was then collected from the inner-side by scrapping using a slide-glass. The small intestinal mucosa from five rats were pooled and weighed. A 3 × volume of 0.15 M KCl (adjusted at pH 7.4 using 0.15 M KOH and 0.15 M HCl) containing 10 mM EDTA 2Na and trypsin inhibitor (0.5 mg ml^{-1}) was added to the small intestinal mucosa and homogenized in an ice bath. The homogenate was centrifuged at 9000*g* for 20 min at 4°C, and an aliquot of the supernatant was further centrifuged at 105 000*g* for 60 min at 4°C. The supernatant, cytosol, was stored at −80°C until use. The remaining pellet fractions were collected, suspended again with 2 ml 100 mM potassium phosphate buffer (pH 7.4) containing trypsin inhibitor (0.5 mg ml^{-1}) and 1 mM EDTA 2Na, and stored at −80°C until use. Proteins were determined by the method of Lowry et al. (1951), with bovine serum albumin as a standard.

In vivo *studies*

OT-7100 was suspended in polyethylene glycol 400 for intravenous administration and in 5% acacia solution for oral administration. The animals were fasted for 20 h before OT-7100 administration. OT-7100 was administered orally at doses of 30, 100 and 1000 mg kg^{-1} to rats, dogs and monkeys, respectively, and intravenously at the same dose of 5 mg kg^{-1} to rats, dogs and monkeys. OT-7100 was administered at 09:00 h. All treated animals were given access to food at 11:00 h and were allowed free access to tap water. Heparinized samples of whole blood were obtained from rats, dogs and monkeys at several time points after administration (Figure 2) (24 h was the last sampling tine after oral and intravenous administration). Plasma samples were separated from whole blood by centrifuging the blood samples at 1800*g* for 10 min at 4°C and were stored frozen at −20°C until the analyses were performed.

OT-7100 and its metabolites in the plasma were assayed using a validated high-performance liquid chromatography (HPLC) method. Briefly, a 0.3-ml aliquot of each plasma sample was first added to 0.9 ml acetonitrile. After centrifugation at 10 000*g* for 15 min at 4°C, the supernatant (0.9 ml) was transferred to another tube and dried under nitrogen at 40°C. The residue was dissolved in 0.5 ml of a mixture of acetonitrile and potassium phosphate buffer (10 mM, pH 5.5) at a ratio of 1:3 (v/v) and 0.2 ml of this suspension were then injected onto the HPLC.

In vitro *metabolic studies of OT-7100*

The hydroxylase activities towards OT-7100 were determined by quantifying the formation of M19 (Figure 1). A 0.1-ml aliquot of cytosol and microsomes from the liver and small intestine of rats, dogs, monkeys and humans (approximately 10 mg protein ml^{-1}) was added to 0.89 ml 0.1 M Na-K phosphate buffer (pH 7.4). The reaction was started by adding 10 µl substrate (1000 µg ml^{-1} acetonitrile) after pre-incubation for 5 min at 37°C. The reaction was stopped by adding 2.0 ml acetonitrile after incubation for 30 min at 37°C. The reaction mixture was then centrifuged at 3000 rpm for 10 min at 4°C. The resulting supernatant (1.0 ml) was evaporated under a nitrogen stream at 40°C. The residue was dissolved in 0.5 ml of a mixture of acetonitrile and potassium phosphate buffer (10 mM, pH 5.5) at a ratio of 1:3 (v/v) and a 0.2-ml aliquot was injected onto the HPLC.

HPLC analysis of OT-7100 and metabolites

OT-7100 and its metabolites were assayed using a HPLC method validated over a concentration range of 0.01–1.00 µg ml^{-1}. OT-7100 and its metabolites were separated on a 250 × 4.6 mm i.d. Inertsil ODS-3V column (GL-Sciences, Tokyo, Japan) and detected at wavelengths of 215 nm (for M19) and 230 nm (for OT-7100 and the other four metabolites) using an HPLC system (LC-10A Series, Shimadzu, Kyoto, Japan). OT-7100 and the metabolites were eluted at a flow rate of 1.0 ml min^{-1} with 10 mM potassium buffer (pH 5.5)/acetonitrile according to the following gradient schedule: 33% acetonitrile for the first 3 min; a linear gradient from 33 to 40% over the next 7 min; a linear gradient from 40 to 50% over the next 4 min; a linear gradient from 50 to 64% over the next 6 min; a linear gradient from 64 to 68% over the next 3 min; and a linear gradient from 68 to 70% over the next 9 min, which was then finally maintained at 80% for 10 min. The temperature of the column was maintained at 40°C.

Data analysis

The OT-7100 concentrations at time 0 (C_0) were extrapolated from the initial slope. The maximum concentrations (C_{max}) and the times to reach the maximum concentration (T_{max}) were read directly from the mean concentration data. The elimination half-lives ($t_{1/2}$) were estimated as $\ln 2/k$, where k is the slope of the terminal linear portion of the semi-logarithmic plasma concentration–time curve. The areas under the plasma concentration–time curves from time 0 to the last detectable concentration (AUC_{0-t}) and the mean residence times (MRT) were calculated using the trapezoidal rule (Yamaoka et al. 1978). Total systemic clearances (CL_{tot}) and volume of distribution at steady state (V_{dss}) were calculated according to the following equations:

$$CL_{tot} = \frac{D_{i.v.}}{AUC_{0-t}}$$

$$V_{dss} = D_{i.v.} \cdot \frac{MRT}{AUC},$$

where $D_{i.v.}$ is the administered dose. The absolute bioavailability (BA) was calculated as:

$$D_{i.v.} \cdot \frac{AUC_{p.o.}}{D_{p.o.}} \cdot AUC_{i.v.}$$

of OT-7100 in the plasma and expressed as a percentage. The AUC_{0-t} values of OT-7100 after oral administration were normalized for the dose levels divided by $mg\,kg^{-1}$.

Statistical analysis

All graphical data are the mean ± SD. Analysis of statistical significance, where appropriate, was performed by the Tukey's test using the statistical package program SAS® System 8.2 (SAS Institute, Inc., Cary, NC, USA).

Results

Species differences in the pharmacokinetics of OT-7100 and its metabolites in rats, dogs and monkeys

The plasma concentration–time profiles of OT-7100 after oral and intravenous administration of OT-7100 to rats, dogs and monkeys are shown in Figure 2 and the pharmacokinetic parameters are summarized in Table I. The plasma concentration–time profiles of OT-7100 were also normalized to a dose of $1\,mg\,kg^{-1}$ (Figure 3).

OT-7100 was administered orally at doses of 30, 100 and $1000\,mg\,kg^{-1}$ to rats, dogs and monkeys, respectively. The C_{max} values for OT-7100 in rats, dogs and monkeys were 0.58, 0.36 and $0.16\,\mu g\,ml^{-1}$, respectively. The $t_{1/2}$ values of OT-7100 in rats, dogs and monkeys were 3.1, 6.2 and 3.6 h, respectively. OT-7100 was not detected in monkey plasma at 24 h after oral administration. The oral bioavailabilities of OT-7100 were calculated from the AUC_{0-t} by normalizing for oral and intravenous administration dose concentrations. The bioavailabilities of OT-7100 in rats, dogs and monkeys were 36, 17 and 0.3%, respectively. In the preliminary experiments, the C_{max} values of OT-7100 in monkey plasma after oral administration increased dose-dependently for doses of $300–1000\,mg\,kg^{-1}$,

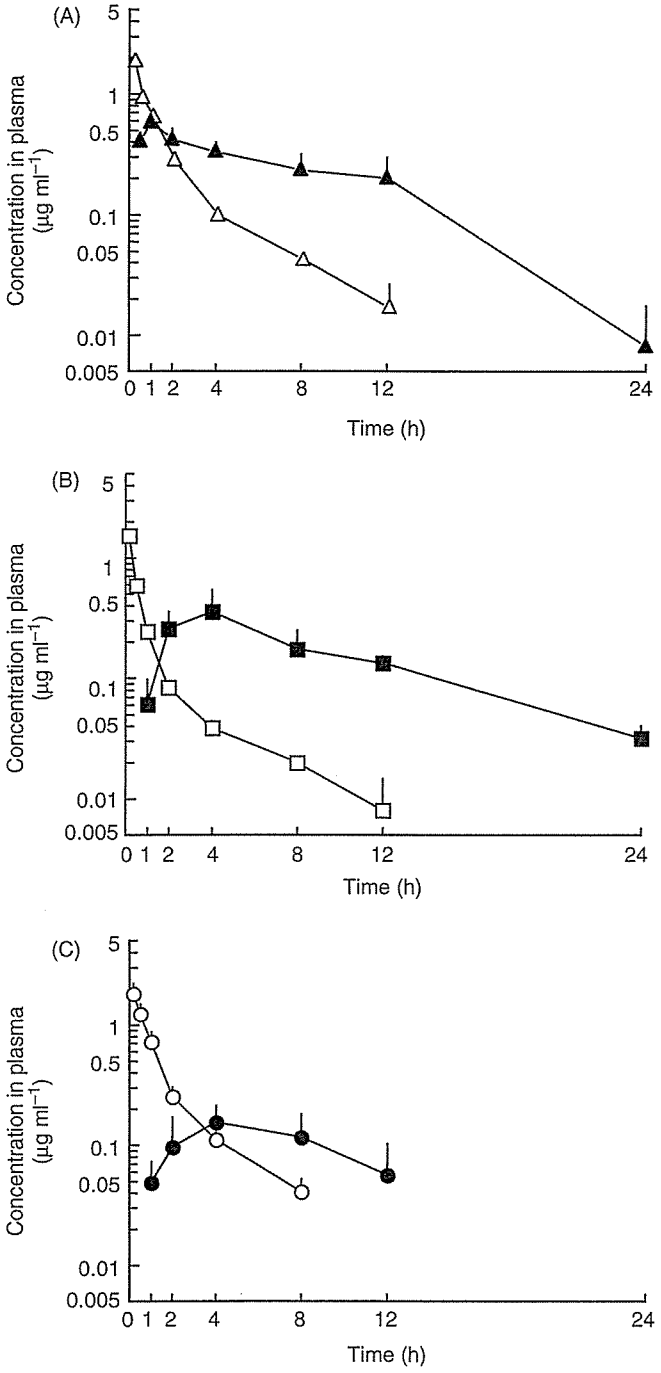

Figure 2. Plasma concentrations of OT-7100 in rats (A), dogs (B) and monkeys (C) after oral (closed symbols) and intravenous (open symbols) administration of OT-7100. OT-7100 was administered orally at a dose of 30 mg kg^{-1} in rats, 100 mg kg^{-1} in dogs and 1000 mg kg^{-1} in monkeys, and intravenously at a dose of 5 mg kg^{-1} in all species. Data are the mean ± SD of three to five animals.

Table I. Pharmacokinetic parameters of OT-7100 in plasma after oral and intravenous administration of OT-7100 to rats, dogs and monkeys.

Species	Rat	Dog	Monkey
Oral administration			
Dose ($mg\,kg^{-1}$)	30	100	1000
C_{max} ($\mu g\,ml^{-1}$)	0.58 ± 0.07	0.36 ± 0.19	0.16 ± 0.06
T_{max} (h)	1.0	4.0	5.3
$t_{1/2}$ (h)	3.1	6.2	3.6
AUC_{0-t} ($\mu g\,h\,ml^{-1}$)	4.88	3.83	1.47
Normalized AUC_{0-t} ($\mu g\,h\,ml^{-1}$)	0.163	0.0383	0.00147
BA (%)	36	17	0.3
Intravenous administration			
Dose ($mg\,kg^{-1}$)	5.0	5.0	5.0
C_0 ($\mu g\,ml^{-1}$)	2.05	2.03	2.13
$t_{1/2}(\alpha)$ (h)	0.6	0.3	0.7
$t_{1/2}(\beta)$ (h)	3.4	3.9	2.4
AUC_{0-t} ($\mu g\,h\,ml^{-1}$)	2.28	1.17	2.51
CL_{tot} ($l\,h^{-1}\,kg^{-1}$)	2.0	3.9	1.9
V_{dss} ($l\,kg^{-1}$)	4.8	7.7	3.8
MRT (h)	2.4	2.1	2.0

C_0, plasma concentration at time 0; C_{max}, maximum concentration; T_{max}, time to maximum concentration; $t_{1/2}$, elimination half-life; AUC_{0-t}, area under the plasma concentration–time curve from 0 to the last measurement point; CL_{tot}, clearance = dose/AUC_{0-t}; V_{dss}, volume of distribution; MRT, mean residence time; BA, bioavailability. Data are calculated from the means obtained from five rats, three dogs and three monkeys. C_{max} is mean ± SD of five rats, three dogs and three monkeys.

and OT-7100 bioavailability was the same for doses of 300–1000 $mg\,kg^{-1}$. OT-7100 concentrations in the plasma normalized for oral administered dose concentrations were highest in rats, moderate in dogs and lowest in monkeys. The OT-7100 AUC_{0-t} values normalized for dose levels in rats, dogs and monkeys were 0.163, 0.0383 and 0.00147 $\mu g\,h\,ml^{-1}$ divided by $mg\,kg^{-1}$, respectively. The normalized AUC_{0-t} values of OT-7100 in monkeys were lower than those in dogs and rats (approximately 1/25 of AUC_{0-t} in dogs and 1/100 of AUC_{0-t} in rats).

After intravenous administration of OT-7100 at a dose of 5 $mg\,kg^{-1}$, the plasma concentration–time profiles of OT-7100 in rats, dogs and monkeys were similar. The C_0 values of OT-7100 in rats, dogs and monkeys were 2.05, 2.03 and 2.13 $\mu g\,ml^{-1}$, respectively. The $t_{1/2}(\alpha)$ values of OT-7100 were 0.6 h in rats and 0.7 h in monkeys. OT-7100 was not detected in the plasma of rats, dogs and monkeys at 24 h and in monkey plasma at 12 h after intravenous administration. The AUC_{0-t} values were 2.28 $\mu g\,h\,ml^{-1}$ in rats and 2.51 $\mu g\,h\,ml^{-1}$ in monkeys. In contrast, the $t_{1/2}(\alpha)$ values (0.3 h) of OT-7100 in dog plasma were half of those in rats and monkeys, indicating that the OT-7100 concentrations in dog plasma were eliminated more rapidly and were lower than those in rats and monkeys. The AUC_{0-t} values (1.17 $\mu g\,h\,ml^{-1}$) of OT-7100 in dog plasma were equivalent to approximately 50% of those for rats and monkeys. The CL_{tot} values of OT-7100 in rats, dogs and monkeys were 2.0, 3.9 and 1.9 $l\,h^{-1}\,kg^{-1}$, respectively. The V_{dss} values of OT-7100 in rats, dogs and monkeys were 4.8, 7.7 and 3.8 $l\,kg^{-1}$, respectively.

As shown in Figure 1, the main metabolic pathway of OT-7100 is hydrolysis of the amide moiety (by esterases) to M19 and M5. In the preliminary experiments, M5 was rapidly converted via phase II metabolism to glucuronide and sulfate conjugates and excreted

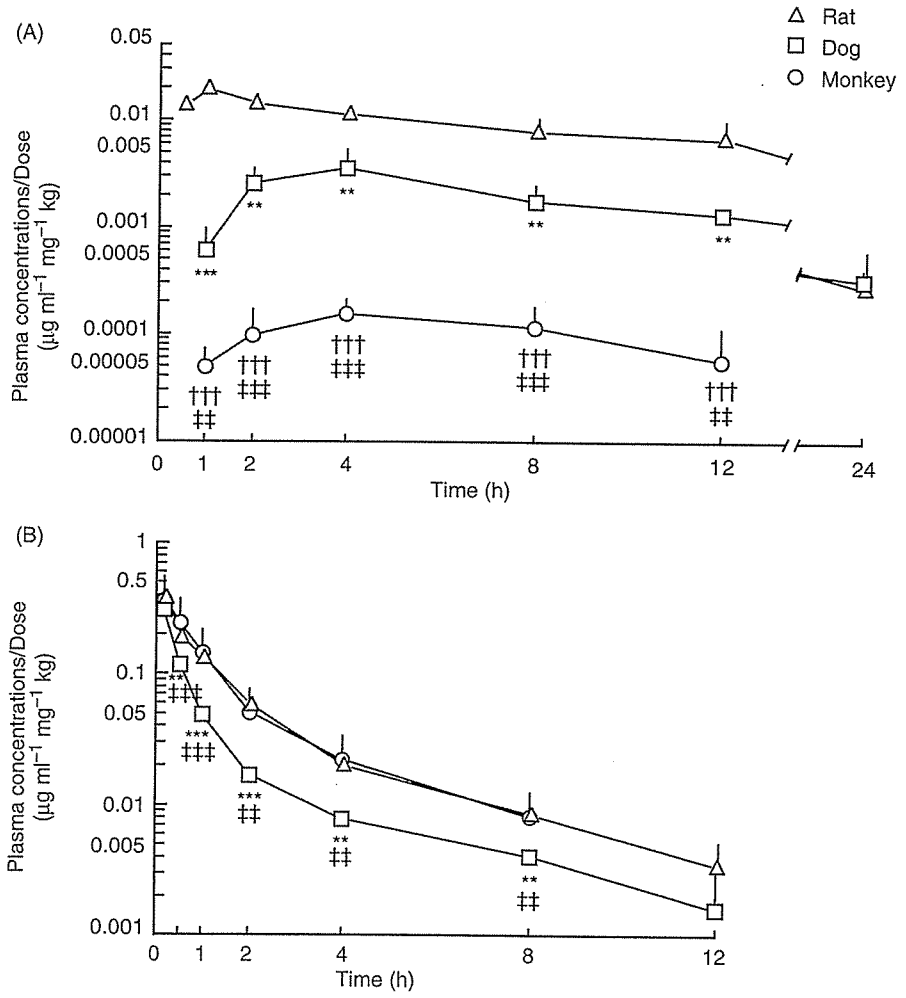

Figure 3. Dose-normalized plasma concentrations–time profiles for OT-7100 in rats, dogs and monkeys after oral (A) and intravenous (B) administration of OT-7100. Data normalized for dose (1 mg kg^{-1}) are expressed as the mean ± SD of three to five animals. Values were significantly different at $^{**}p < 0.01$ and $^{***}p < 0.001$ between rat and dog, at $\dagger\dagger\dagger p < 0.001$ between rat and monkey, and at $\ddagger\ddagger p < 0.01$ and $\ddagger\ddagger\ddagger p < 0.001$ between dog and monkey.

into urine and bile, respectively (data not shown). Since M19 does not readily undergo phase II metabolism (data not shown), it is reasonable to estimate the hydrolase activities toward OT-7100 by quantifying this metabolite. The AUC_{0-t} values of OT-7100 and metabolites are summarized in Table II. After intravenous administration in rats, the AUC_{0-t} values of M19 (formed by hydrolysis of the OT-7100 amide moiety, 10.7 nmol h ml^{-1}) were 1.8 times higher than OT-7100 values. In contrast, after oral administration at a dose of 30 mg kg^{-1} in rats, the AUC_{0-t} values of M19 (66.9 nmol h ml^{-1}) were 5.3 times higher than OT-7100 values. Thus, M19 was determined to be the major metabolite of OT-7100 in rat plasma. In rats, in addition to M19, small amounts of M5 (formed by hydrolysis of the OT-7100 amide moiety) and M1–3 (formed by oxidation of the *n*-butyl groups) were also detected in the plasma. On the other hand, after intravenous

Table II. AUC_{0-t} values of OT-7100 and metabolites in plasma after oral and intravenous administration of OT-7100 to rats and dogs.

Species	Rat	Dog
Oral administration		
Dose ($mg\,kg^{-1}$)	30	100
AUC_{0-t} ($nmol\,h\,ml^{-1}$)		
OT-7100	12.7	10.0
M19	66.9	1812.6
M1	17.7	5.1
M2	3.9	8.8
M3	1.8	n.d.
M5	n.d.	n.d.
Intravenous administration		
Dose ($mg\,kg^{-1}$)	5	5
AUC_{0-t} ($nmol\,h\,ml^{-1}$)		
OT-7100	5.9	3.0
M19	10.7	190.9
M1	2.5	n.d.
M2	0.6	0.5
M3	0.1	n.d.
M5	0.2	n.d.

Metabolite concentrations in monkey plasma were not determined. Data are means obtained from five rats and three dogs. n.d., Not detected.
Molecular weight: M19, 212.20; M1, 416.44; M2, 400.44; M3, 400.44; M5, 190.25.

administration at a dose of $5\,mg\,kg^{-1}$ to dogs, the AUC_{0-t} values of M19 were 190.9 $nmol\,h\,ml^{-1}$, 63.6 times higher than OT-7100 values. After oral administration to dogs, the AUC_{0-t} values of M19 were 1812.6 nmol h ml^{-1}, and were 181.3 times higher than OT-7100 values. Therefore, M19 was also the major metabolite of OT-7100 in dog plasma (Table II).

Comparison of hydrolase activities toward OT-7100 in the liver and small intestine of rats, dogs, monkeys and humans

To elucidate species difference in the hydrolysis of OT-7100, an *in vitro* metabolic study was conducted using liver and small intestinal fractions obtained from rats, dogs, monkeys and humans. Since M19 was determined to be the major OT-7100 metabolite in rats and dogs, hydrolase activities toward OT-7100 were measured based on M19 production (Figure 4).

The hydrolase activities in liver cytosol were similar in all species ($4.6\,ng\,mg\,protein^{-1}\,min^{-1}$ in humans; $3.6–3.8\,ng\,mg\,protein^{-1}\,min^{-1}$ in other animals), indicating that there were no species differences in the hydrolysis of OT-7100 in liver cytosol. In contrast, the hydrolase activities in liver microsomes were 14.8, 19.7 and $14.7\,ng\,mg\,protein^{-1}\,min^{-1}$ in rats, dogs and monkeys, respectively. In human liver microsomes, the hydrolase activity ($4.3\,ng\,mg\,protein^{-1}\,min^{-1}$) was lower than those in the other animal species.

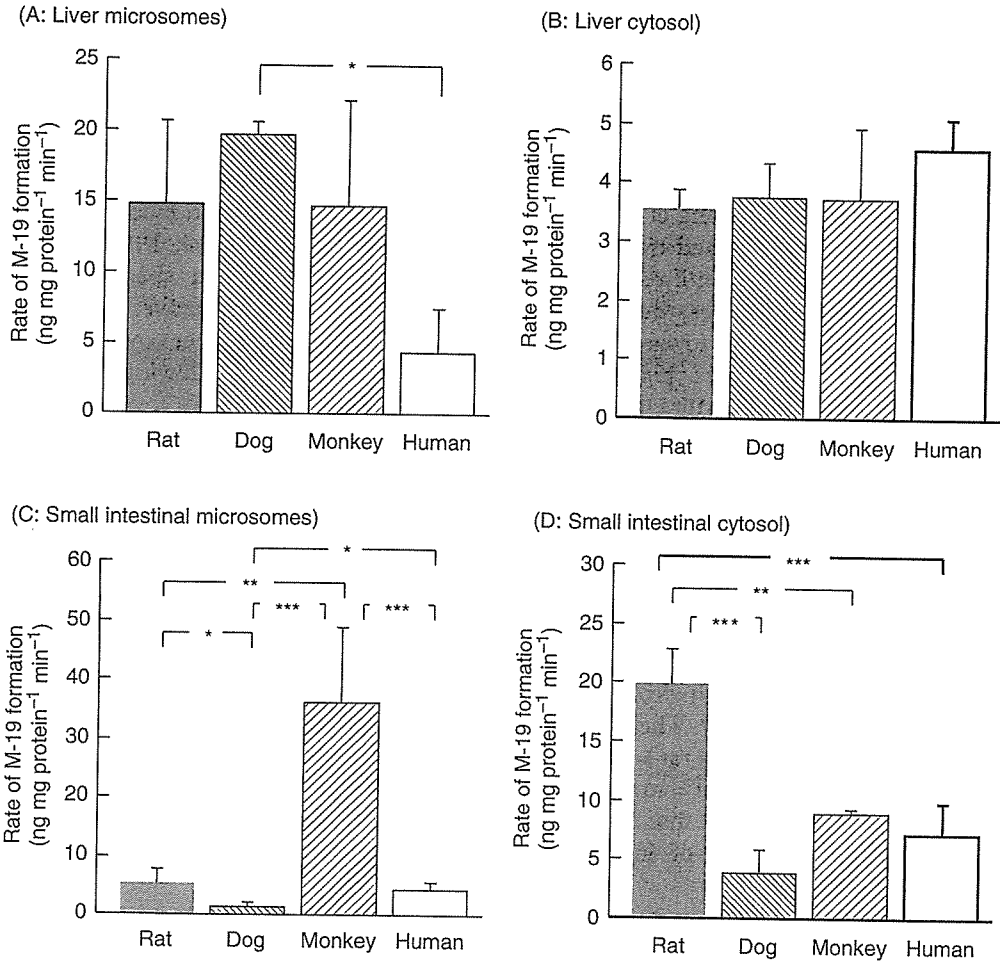

Figure 4. Hydrolase activities toward OT-7100 in liver and small intestinal fractions from rats, dogs, monkeys and humans. Data are the mean ± SD of three lots for rat small intestinal fractions (one lot was prepared from five animals) and three individuals for other fractions. The bracketed pairs of values are significantly different at $*p<0.05$, $**p<0.01$ and $***p<0.001$.

The small intestinal cytosolic hydrolase activities towards OT-7100 in rats (20.0 ng mg protein^{-1} min^{-1}) were significantly the highest, followed by monkeys, humans and dogs. The hydrolase activities determined using small intestinal microsomes from monkeys were 36.1 ng mg protein^{-1} min^{-1}, and were approximately eight, seven and 26 times higher than humans, rats and dogs, respectively. The hydrolase activities toward OT-7100 in dog small intestinal cytosol were approximately one-fifth of those in rats.

Discussion

It is important that first-pass metabolism influences are fully determined to estimate properly the biotransformation of orally administered drugs. The influence of the first-pass

effect in small intestines was investigated herein using OT-7100, a pyrazolopyrimidine derivative, as a probe drug with the amide moiety.

Carboxylesterases play an important role in the metabolic activation of prodrugs and can be classified into four families: CES 1–4 (Satoh and Hosokawa 1998). Various carboxylesterases are expressed in a wide variety of organs and tissues such as the liver, plasma, lung, kidney and brain in addition to the small intestine (Boogaard et al. 1999; Hosokawa et al. 2001; Zhang et al. 2002). Hydrolase activities can be induced by treatment with chemicals and inhibited by a variety of compounds (Morgan et al. 1994a; Yan et al. 1999; Zhu et al. 2000). Until recently, there were only a few reports on species differences in liver hydrolase activities, but the data now available are informative. For example, the hydrolase activities toward *para*-nitrophenylacetate in rat liver microsomes are approximately three times higher than those of dogs in the following order: rat $\geq$ monkey = human > dog (Morgan et al. 1994b). The hydrolase activities toward isocarboxazid in monkey liver microsomes are approximately 2.5 times higher than those of rats in the following order: monkey > dog $\geq$ rat > human. Moreover, the hydrolase activities toward butanilicaine in dog liver microsomes are approximately nine times higher than rats (Hosokawa et al. 1990). The hydrolase activities toward *O*-butyryl propranolol in dog liver microsomes are approximately twice higher than those of rats (Imai et al. 2003). Therefore, species differences in hydrolase activities by esterases differ widely from substrate to substrate.

In the present study, the hydrolase activities toward OT-7100 in liver cytosol were similar in all species tested. The hydrolyzing activities in dog liver microsomes were higher than those in rats and monkeys. The *in vitro* hydrolase activities in liver microsomes correlated with CL_{tot} and V_{dss} (dog > rat = monkey; Table I), and inversely correlated with OT-7100 plasma concentrations (rat = monkey > dog; Figure 3A) after intravenous administration. These result demonstrate that hydrolysis in the liver is one of the major contributions to the biotransformation of intravenously administered drugs with the amide moiety such as OT-7100.

Compared with data on carboxylesterases in the liver, there are few reports on species differences for hydrolysis by carboxylesterases in the small intestine. Inoue et al. (1979) examined hydrolase activities for several substrates using homogenates of intestinal mucosa from six species (human, rat, mouse, guinea pig, rabbit and dog), and reported a difference in the substrate specificity of the intestinal esterase from mice and rats, which hydrolysed esters better compared with the other species. The same study reported that hydrolase activities from dog intestine, tested using several esters as substrates, were low (Inoue et al. 1979). Furthermore, the *in vitro* hydrolysis rate in small intestinal mucosa for glycovir, a perbutyrylated ester prodrug of SC-48334, was highest in rats, moderate in monkeys and humans, and lowest in dogs, which was also reflected in the order of decreasing relative bioavailability of active SC-48334 (Cook et al. 1995).

In the present study, hydrolase activities toward OT-7100 in small intestinal cytosol were highest in rats, moderate in monkeys and humans, and lowest in dogs, consistent with Cook et al. (1995). In contrast, our findings on the rank order of hydrolase activities in small intestinal microsomes are not consistent with previous studies. The hydrolase activities in small intestinal microsomes from monkeys were seven, eight and 26 times higher than those of rats, humans and dogs, respectively. Therefore, species differences in hydrolase activities in the small intestinal microsomes varied more widely compared with those within the liver.

The results also demonstrate that the highest activity of OT-7100 hydrolysis in small intestinal microsomes from monkeys is one factor accounting for the poor oral bioavailability

in monkeys (0.3%). This conclusion is also supported by the species differences observed in OT-7100 plasma concentration–time profiles normalized for dose concentration after oral administration (Figure 3B) (rat > dog ≫ monkey). Therefore, the present results verify that hydrolase activity in the small intestine in the process of absorption plays an important role in small intestinal first-pass metabolism after oral administration of a drug bearing an amide moiety. Furthermore, since the carboxylesterase isoform present in the small intestine is different from that in the liver and that OT-7100 is a good substrate for the carboxylesterase isoforms in monkey small intestines.

Since there are marked species variations in substrate specificity and tissue distribution of carboxylesterases, it is not yet possible to predict using animal studies all relevant aspects of drug metabolism and pharmacokinetics in human clinical studies involving administration of drugs with an amide moiety. However, the results presented here offer an important index to extrapolate drug metabolism and pharmacokinetics in humans from *in vitro* studies using both human and animal tissue fractions as well as animal studies. Particularly relevant is the observation that hydrolase activities toward OT-7100 in human liver microsomes were one-third to one-fifth lower than those in other species (Figure 4). Therefore, after intravenous administration to humans, OT-7100 should have a longer half-life and lower clearance in humans than in other animals. Our data indicate that the metabolism and pharmacokinetics of OT-7100 in humans would be sufficiently different such that the predicted bioavailabilities of this drug in humans would be higher than those in monkeys. In fact, it was confirmed that the plasma concentrations of OT-7100 in human volunteers normalized for dose concentration after oral administration were higher than those of monkeys (data not shown).

In conclusion, this paper has demonstrated that small intestinal hydrolysis in the process of absorption plays a crucial role in the first-pass metabolism of the OT-7100 after oral administration. Furthermore, OT-7100 is a good substrate for esterase isoforms in monkey small intestine and can therefore be a good probe drug to elucidate differences in small intestinal hydrolase activities between humans and monkeys. This information provides an important index for extrapolating human drug pharmacokinetics from preclinical monkey studies.

References

Boogaard PJ, Van Elburg PA, De Kloe KP, Watson WP, Van Sittert NJ. 1999. Metabolic inactivation of 2-oxiranylmethyl 2-ethyl-2,5-dimethylhexanoate (C10GE) in skin, lung and liver of human, rat and mouse. Xenobiotica 29:987–1006.

Boxenbaum H. 1980. Interspecies variation in liver weight, hepatic blood flow, and antipyrine intrinsic clearance: Extrapolation of data to benzodiazepines and phenytoin. Journal of Pharmacokinetics and Biopharmaceutics 8:165–176.

Campbell CJ, Chantrell LJ, Eastmond R. 1987. Purification and partial characterization of rat intestinal cefuroxime axetil esterase. Biochemical Pharmacology 36:2317–2324.

Cook CS, Karabatsos PJ, Schoenhard GL, Karim A. 1995. Species dependent esterase activities for hydrolysis of an anti-HIV prodrug glycovir and bioavailability of active SC-48334. Pharmaceutical Research 12:1158–1164.

Fitzsimmons ML, Collins JM. 1997. Selective biotransformation of the human immunodeficiency virus protease inhibitor Saquinavir by human small-intestinal cytochrome P4503A4. Potential contribution to high first-pass metabolism. Drug Metabolism and Disposition 25:256–266.

Hashizume T, Imaoka S, Mise M, Terauchi Y, Fujii T, Miyazaki H, Kamataki T, Funae Y. 2001. Involvement of CYP2J2 and CYP4F12 in the metabolism of ebastine in human intestinal microsomes. Journal Pharmacology and Experimental Therapeutics 300:298–304.

Hosokawa M, Endo T, Fujisawa M, Hara S, Iwata N, Sato Y, Satoh T. 1995. Interindividual variation in carboxylesterase levels in human liver microsomes. Drug Metabolism and Disposition 23:1022–1027.

Hosokawa M, Maki T, Satoh T. 1990. Characterization of molecular species of liver microsomal carboxylesterases of several animal species and humans. Archives of Biochemistry and Biophysics 277:219–227.

Hosokawa M, Suzuki K, Takahashi D, Mori M, Satoh T, Chiba K. 2001. Purification, molecular cloning, and functional expression of dog liver microsomal acyl-CoA hydrolase: A member of the carboxylesterase multigene family. Archives of Biochemistry and Biophysics 389:245–253.

Imai T, Yoshigae Y, Hosokawa M, Chiba K, Otagiri M. 2003. Evidence for the involvement of a pulmonary first-pass effect via carboxylesterase in the disposition of a propranolol ester derivative after intravenous administration. Journal of Pharmacology and Experimental Therapeutics 307:1234–1242.

Inaba M, Ohnishi Y, Ishii H, Tanioka Y, Yoshida Y, Sudoh K, Hakusui H, Mizuno N, Ito K, Sugiyama Y. 1998. Pharmacokinetics of CPT-11 in rhesus monkeys. Cancer Chemotherapy and Pharmacology 41:103–108.

Inoue M, Morikawa M, Tsuboi M, Sugiura M. 1979. Species difference and characterization of intestinal esterase on the hydrolyzing activity of ester-type drugs. Japanese Journal of Pharmacology 29:9–16.

Lin JH. 1995. Species similarities and differences in pharmacokinetics. Drug Metabolism and Disposition 23:1008–1021.

Lin JH, Chiba M, Baillie TA. 1999. Is the role of the small intestine in first-pass metabolism overemphasized? Pharmacological Reviews 51:135–158.

Lowry OH, Rosebrough NJ, Farr AL, Randall RJ. 1951. Protein measurement with the Folin phenol reagent. Journal of Biological Chemistry 193:264–275.

Miki S, Yoshinaga N, Iwamoto T, Yasuda T, Sato S. 2001. Antinociceptive effect of the novel compound OT-7100 in a diabetic neuropathy model. European Journal of Pharmacology 430:229–234.

Morgan EW, Yan B, Greenway D, Parkinson A. 1994a. Regulation of two rat liver microsomal carboxylesterase isozymes: Species differences, tissue distribution, and the effects of age, sex, and xenobiotic treatment of rats. Archives of Biochemistry and Biophysics 315:513–526.

Morgan EW, Yan B, Greenway D, Peterson DR, Parkinson A. 1994b. Purification and characterization of two rat liver microsomal carboxylesterases (hydrolase A and B). Archives of Biochemistry and Biophysics 31:495–512.

Satoh T. 1987, Role of carboxylesterases in xenobiotic metabolism. In: Bend JR, Hodgson E, Philpot RM, editors. New York, NY: Elsevier. pp 155–181.

Satoh T, Hosokawa M. 1998. The mammalian carboxylesterases: From molecules to functions. Annual Review of Pharmacology and Toxicology 38:257–288.

Thummel KE, Kunze KL, Shen DD. 1997. Enzyme-catalyzed processes of first-pass hepatic and intestinal drug extraction. Advanced Drug Delivery Reviews 27:99–127.

Thummel KE, O'Shea D, Paine MF, Shen DD, Kunze KL, Perkins JD, Wilkinson GR. 1996. Oral first-pass elimination of midazolam involves both gastrointestinal and hepatic CYP3A-mediated metabolism. Clinical Pharmacology and Therapeutics 59:491–502.

Yamaoka K, Nakagawa T, Uno T. 1978. Statistical moments in pharmacokinetics. Journal of Pharmacokinetics and Biopharmaceutics 6:547–558.

Yan B, Matoney L, Yang D. 1999. Human carboxylesterases in term placentae: Enzymatic characterization, molecular cloning and evidence for the existence of multiple forms. Placenta 20:599–607.

Yasuda T, Iwamoto T, Ohara M, Sato S, Kohri H, Noguchi K, Senba E. 1999. The novel analgesic compound OT-7100 (5-nButyl-7-(3,4,5,-trimethoxybenzoylamino)pyrazolo[1,5-a]pyrimidine) attenuates mechanical nociceptive responses in animal models of acute and peripheral neuropathic hyperalgesia. Japanese Journal of Pharmacology 79:65–73.

Yasuda T, Okamoto K, Iwamoto T, Miki S, Yoshinaga N, Sato S, Noguchi K, Senba E. 2001. A novel analgesic compound OT-7100 attenuates nociceptive responses in animal models of inflammatory and neuropathic hyperalgesia: A possible involvement of adenosinergic anti-nociception. Japanese Journal of Pharmacology 87:214–225.

Zhang QY, Dunbar D, Ostrowska A, Zeisloft S, Yang J, Kaminsky LS. 1999. Characterization of human small intestinal cytochromes P-450. Drug Metabolism and Disposition 27:804–809.

Zhang W, Xu G, McLeod HL. 2002. Comprehensive evaluation of carboxylesterase-2 expression in normal human tissues using tissue array analysis. Applied Immunohistochemistry and Molecular Morphology 10:374–380.

Zhu W, Song L, Zhang H, Matoney L, Lecluyse E, Yan B. 2000. Dexamethasone differentially regulates expression of carboxylesterase genes in humans and rats. Drug Metabolism and Disposition 28:186–191.

0026-895X/06/7002-477–486$20.00
MOLECULAR PHARMACOLOGY

Mol Pharmacol 70:477–486, 2006

Vol. 70, No. 2
22673/3125134
Printed in U.S.A.

CYP2C76, a Novel Cytochrome P450 in Cynomolgus Monkey, Is a Major CYP2C in Liver, Metabolizing Tolbutamide and Testosterone

Yasuhiro Uno, Hideki Fujino, Go Kito, Tetsuya Kamataki, and Ryoichi Nagata

Laboratories of Translational Research (Y.U., G.K., R.N.) and Drug Metabolism (T.K.), Graduate School of Pharmaceutical Sciences, Hokkaido University, Hokkaido, Japan; Shin Nippon Biomedical Laboratories, Tokyo, Japan (Y.U., G.K., R.N.); and Tokyo New Drug Research Laboratories I, Kowa Co., Tokyo, Japan (H.F.)

Received January 20, 2006; accepted April 21, 2006

ABSTRACT

Monkeys are widely used as a primate model to study drug metabolism because they generally show a metabolic pattern similar to humans. However, the paucity of information on cytochrome P450 (P450) genes has hampered a deep understanding of drug metabolism in the monkey. In this study, we report identification of the CYP2C76 cDNA newly identified in cynomolgus monkey and characterization of this CYP2C along with cynomolgus CYP2C20, CYP2C43, and CYP2C75. The CYP2C76 cDNA contains the open reading frame encoding a protein of 489 amino acids that are only approximately 80% identical to any human or monkey P450 cDNAs. Gene and protein expression of CYP2C76 was confirmed in the liver of cynomolgus and rhesus monkeys but not in humans or the great apes. Moreover, *CYP2C76* is located at the end of the *CYP2C* gene cluster in the monkey genome, the region of which corresponds to the intergenic region adjacent to the *CYP2C* cluster in the human genome, strongly indicating that this gene does not have the ortholog in humans. Among the four *CYP2C* genes expressing predominantly in the liver, the expression level of *CYP2C76* was the greatest, suggesting that CYP2C76 is a major CYP2C in the monkey liver. Assays for the capacity of CYP2C76 to metabolize drugs using several substrates typical for human CYP2Cs revealed that CYP2C76 showed unique metabolic activity. These results suggest that CYP2C76 contributes to overall drug-metabolizing activity in the monkey liver and might account for species difference occasionally seen in drug metabolism between monkeys and humans.

Cytochrome P450s (P450s) are one of the most important drug-metabolizing enzymes and form a superfamily consisting of a large number of subfamilies (Nelson et al., 1996, 2004). The cDNA sequences encoding P450s have been reported for many species of not only mammals but also birds, insects, plants, bacteria, and others (see http://drnelson.utmem.edu/CytochromeP450.html). In humans, 57 functional genes have been identified to date (Nelson et al., 2004). The human CYP2C subfamily, comprising CYP2C8, CYP2C9, CYP2C18, and CYP2C19, is essential in metabolizing approximately 20% of all prescribed drugs, including tolbutamide, phenytoin, warfarin, and ibuprofen (Goldstein, 2001). The CYP2C subfamily consists of multiple members in each mammalian species, including 15 in mice, 12 in rats, and 9 in rabbits (for the latest information, see http://drnelson.utmem.edu/CytochromeP450.html). Between humans and rodents, the number of the subfamily members is different, and none of the CYP2Cs seems to show a clear orthologous relationship between the two species, suggesting that the data from rodents must be cautiously interpreted and extrapolated to humans (Nelson et al., 2004).

For monkeys, which generally mean Old or New World monkeys, three CYP2C cDNAs have been identified in the macaque and cynomolgus (*Macaca fascicularis*) and rhesus (*Macaca mulatta*) monkeys. Two sequences have been published including cynomolgus CYP2C20 (Komori et al., 1992) and rhesus CYP2C43 (Matsunaga et al., 2002), whereas rhesus CYP2C75 has been reported to GenBank but unpublished. CYP2C20 shows ~95% homology to human CYP2C8, whereas CYP2C43 and CYP2C75 have ~95% identity to both human CYP2C9 and CYP2C19. Among these monkey CYP2Cs, only CYP2C43 has been analyzed for drug-metabolizing capacity using the recombinant protein, showing activities toward *S*-mephenytoin but not tolbutamide, similar

Article, publication date, and citation information can be found at http://molpharm.aspetjournals.org.
doi:10.1124/mol.106.022673.

ABBREVIATIONS: P450, cytochrome P450; PCR, polymerase chain reaction; BAC, bacterial artificial chromosome; RT, reverse transcription; TLC, thin-layer chromatography; PDI, protein disulfide isomerase; EST, expressed sequence tag; PTC, premature termination codon; NMD, nonsense-mediated decay.